Journal of Computer-Aided Molecular Design, **14:** 147–160, 2000.
KLUWER/ESCOM

Automated docking and molecular dynamics simulations of nimesulide in the cyclooxygenase active site of human prostaglandin-endoperoxide synthase-2 (COX-2)

Raquel García-Nieto, Carlos Pérez & Federico Gago*
Departamento de Farmacología, Universidad de Alcalá, E-28871 Alcalá de Henares, Madrid, Spain

Received 29 March 1999; Accepted 7 July 1999

Key words: cyclooxygenases, continuum electrostatics, docking, molecular dynamics, molecular modeling, NSAIDs, prostaglandins

Summary

Molecular models of the complex between the selective COX-2 inhibitor nimesulide and the cyclooxygenase active site of human prostaglandin-endoperoxide synthase-2 have been built using a combination of homology modelling, conformational searching and automated docking techniques. The stability of the resulting complexes has been assessed by molecular dynamics simulations and interaction energy decomposition. It is found that nimesulide exploits the extra space made available by the replacement at position 523 of an isoleucine residue in COX-1 by a valine in COX-2 and establishes electrostatic interactions with both Arg-106 and Arg-499 (Arg-120 and Arg-513 in PGHS-1 numbering). Two alternate binding modes are proposed which are compatible with the pharmacological profile of this agent as a COX-2 selective inhibitor.

Introduction

Prostaglandin-endoperoxide synthase (PGHS) is a bifunctional enzyme which first converts arachidonic acid into prostaglandin G_2 (PGG_2) by dioxygenation, and then catalyzes the peroxidation of PGG_2 to PGH_2, the precursor to the formation of several important mediators of pain, fever, and inflammation collectively called prostanoids. Inhibition of the cyclooxygenase (COX) activity of PGHS can be achieved by the widely used pharmacological class of non-steroidal antiinflammatory agents (NSAIDs) [1].

Two isoforms of PGHS have been identified, sequenced and cloned. PGHS-1 (also known as COX-1) is a constitutive enzyme involved in the regulation of many cellular processes including vascular homeostasis, gastrointestinal cytoprotection, and renal function. PGHS-2 (or COX-2) is mostly an inducible form that is expressed in inflamed tissue or following exposure to growth factors, lymphokines, and other stimuli, and has been implicated not only in inflammation but also in cancer and neurodegenerative diseases [1].

Both PGHS-1 and PGHS-2 are integral membrane proteins found on the lumenal surfaces of the endoplasmic reticulum and within the nuclear envelope of different cell types [2]. Despite the similar subcellular location and the overall sequence similarity (Figure 1), biochemical and pharmacological differences exist between the two isoforms. For example, PGHS-2 accepts a wider range of fatty acids as substrates than does PGHS-1, and when acetylated by aspirin on Ser-530, PGHS-1 does not oxidize arachidonic acid whereas similarly acetylated PGHS-2 will still function as a 15-lipoxygenase, oxidizing arachidonic acid to 15(*R*)-hydroxy-eicosatetraenoic acid (15-HETE) [3]. As regards inhibition by NSAIDs, both isoforms can be inhibited to a larger or lesser extent but some compounds are more selective than others [4, 5]. A slow conversion between an initial reversible complex and a functionally irreversible one is thought to be responsible for the selectivity of inhibition of PGHS-2 over PGHS-1 [6]. Since inhibition of PGHS-2 alone may

*To whom correspondence should be addressed. E-mail: fgago@fisfar.alcala.es.

```
            85                                                  128  146    153
PGH1_SHEEP   SPSFIHFMLTHGRWLWDFVN-ATFIRDTLMRLVLTVRSNLIPSPP....VSYYTRIL...
PGH1_HUMAN   SPSFTHFLLTHGRWFWEFVN-ATFIREMLMRLVLTVRSNLIPSPP....VSYYTRIL...
PGH2_MOUSE   TPNTVHYILTHFKGVWNIVNNIPFLRSLIMKYVLTSRSYLIDSPP....LSYYTRAL...
PGH2_HUMAN   TPNTVHYILTHFKGFWNVVNNIPFLRNAIMSYVLTSRSHLIDSPP....LSYYTRAL...
             *=***=**=====** =* ==***=*=  *= *===*== ==*===    *=====*=
            181                                                 229
PGH1_SHEEP   RFLLRRKFIPDPQGTNLMFAFFAQHFTHQFFKTSGKMGPGFTKALGHGVD
PGH1_HUMAN   RFLLRRKFIPDPQGTNLMFAFFAQHFTHQFFKTSGKMGPGFTKALGHGVD
PGH2_MOUSE   KVLLRREFIPDPQGSNMMFAFFAQHFTHQFFKTDHKRGPGFTRGLGHGVD
PGH2_HUMAN   KLLLRRKFIPDPQGSNMMFAFFAQHFTHQFFKTDHKRGPAFTNGLGHGVD
             * ==== =======*=*================**=*== == *======
            338                                                 392
PGH1_SHEEP   GETIKIVIEEYVQQLSGYFLQLKFDPELLFGAQFQYRNRIAMEFNQLYHWHPLMP
PGH1_HUMAN   GETIKIVIEEYVQQLSGYFLQLKFDPELLFGVQFQYRNRIAMEFNHLYHWHPLMP
PGH2_MOUSE   GETIKIVIEDYVQHLSGYHFKLKFDPELLFNQQFQYQNRIASEFNTLYHWHPLLP
PGH2_HUMAN   GETIKIVIEDYVQHLSGYHFKLKFDPELLFNKQFQYQNRIAAEFNTLYHWHPLLP
             =========*===**===***==========* ====*==== ===*=======*=
            429
PGH1_SHEEP   QPAGRIGGGRNIDHHILHVAVDVIKESRVLRLQPFNEYRKRFGMKPYTSFQELTGEKEMAAELEEL
PGH1_HUMAN   QIAGRIGGGRNMDHHILHVAVDVIRESREMRLQPFNEYRKRFGMKPYTSFQELVGEKEMAAELEEL
PGH2_MOUSE   QIAGRVAGGRNVPIAVQAVAKASIDQSREMKYQSLNEYRKRFSLKPYTSFEELTGEKEMAAELKAL
PGH2_HUMAN   QIAGRVAGGRNVPPAVQKVSQASTDQSRQMKYQSFNEYRKRFMLKPYESFEELTGEKEMSAELEAL
             =*===**====** *** =  ** **== ***=* ======= *=== ==*==*===== === *=
                                                    537   559  564   578 582
PGH1_SHEEP   YGDIDALEFYPGLLLEKCHPNSIFGESMIEMGAPFSLKGLLGN.....VKTATL.....VSFHV...
PGH1_HUMAN   YGDIDALEFYPGLLLEKCHPNSIFGESMIEIGAPFSLKGLLGN.....VKTATL.....VSFRV...
PGH2_MOUSE   YSDIDVMELYPALLVEKPRPDAIFGETMVELGAPFSLKGLMGN.....INTASI.....TSFNV...
PGH2_HUMAN   YGDIDAVELYPALLVEKPRPDAIFGETMVEVGAPFSLKGLMGN.....INTASI.....TSFSV...
             = ===  =*==*==*==**=**====*=*= =========*==     **==**     *== =
```

Figure 1. Alignment [61] of mouse and human PGHS-2 residues used in model construction. Residue numbering follows the convention for the sheep PGHS-1 structure (PDB entry 1prh). An asterisk under a given amino acid means identity in that position for mouse and human PGHS-2 enzymes; the = sign stands for a conserved residue in both PGHS-1 and PGHS-2 isozymes from the three species. The valine that occupies the same position as Ile-523 in PGHS-1 and the arginine that replaces His-513 are highlighted in bold type.

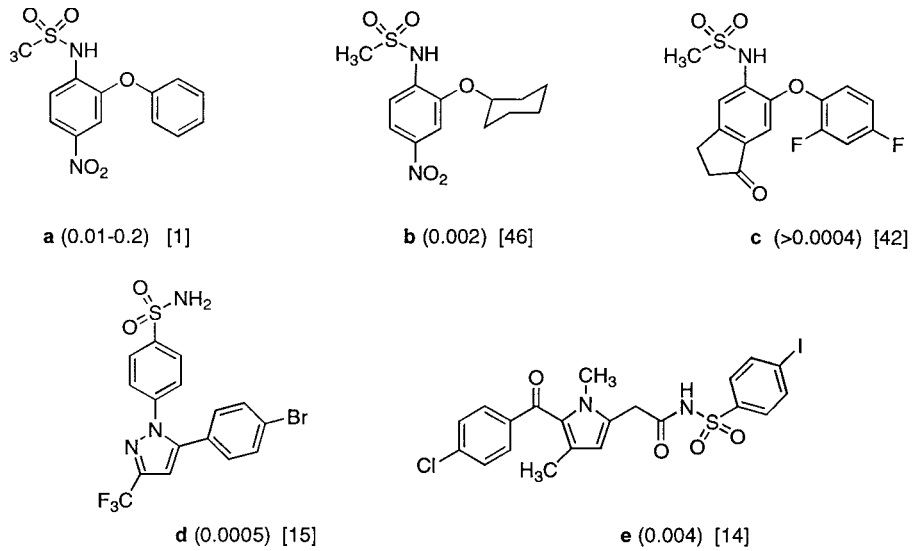

Figure 2. Chemical structures of (a) nimesulide, (b) NS-398, (c) flosulide, (d) SC-558, and (e) RS-104897. Selectivity ratios of COX-2/COX-1 inhibition are given in parentheses although these numbers can vary greatly depending on assay conditions [1].

be sufficient to obtain an antiinflammatory effect and most mechanism-based side effects result from blockade of PGHS-1 activity in normal tissues, targeting this second isoform has stimulated renewed interest in the field of NSAIDs with the aim of developing new agents with an improved safety profile. In fact, several classes already exist of compounds that display such selectivity, and many of them have in common the presence of two appropriately substituted aromatic rings on adjacent positions about a central, usually heterocyclic ring [7–9]. More recently, a novel class of aspirin-based covalent inhibitors, such as o-(acetoxyphenyl)hept-2-ynyl sulfide, has also been developed which lead to potent and irreversible inactivation of COX-2 [10].

The structure-based design of novel NSAIDs gained important impetus when the complexes of PGHS-1 from ram seminal vesicles with several inhibitors were crystallized and solved by X-ray diffraction techniques [11–13]. This seminal work paved the way to the successful crystallization of human [14] and mouse PGHS-2 [15] in the presence of selective and non-selective inhibitors. Despite this wealth of structural information, the aspects of the drug-enzyme interaction that determine the COX-2 selectivity of certain NSAIDs are not always clear as in some cases there appear to be no direct ligand-protein interactions with amino acid residues that are unique to COX-2 [14, 16].

Nimesulide (4-nitro-2-phenoximethanesulfonanilide; Figure 2) [17] is a prototype of relatively selective COX-2 inhibitor [18–20] in current therapeutic use [21]. Remarkably, it was already on the market as an antiinflammatory agent without the gastrointestinal side effects of classical NSAIDs prior to the discovery of the inducible COX isoform [1]. In fact, a selectivity of this drug towards the PGHS involved in inflammation was suggested more than twenty years ago when a lack of correlation was found between its potency to inhibit PGHS in preparations from bovine seminal vesicles and its antiinflammatory potency in vivo, which was comparable to that of indomethacin [22].

In the present paper we address the mode of interaction of nimesulide with the cyclooxygenase active site of human PGHS-2 (hPGHS-2) making use of automated docking methods and molecular dynamics simulations [23].

Methodology

hPGHS-2 model building and energy refinement

The three-dimensional structure of uninhibited mouse PGHS-2 [15], retrieved from the Protein Data Bank (PDB) [24], formed the basis of our homology modelling [25] of its human counterpart, which has been solved [14] but is not publicly available. Mouse and human PGHS-2 have 604 amino acid residues each and they share almost 90% sequence identity. For the present work we focused on a reduced model of the cyclooxygenase active site that comprises the three helices making up the membrane binding domain and all those residues within 20 Å of the substrate binding channel (Figure 1). The number of fragments was kept to a minimum by including some additional connecting residues, and the resulting peptide chains were capped with suitable acetyl and N-methyl groups in place of the preceding and following amino acids, respectively. Hydrogens were added using standard geometries and their positions were optimized using the molecular mechanics program AMBER [26] and a dielectric constant $\epsilon = 4r_{ij}$ including all atom pairs in the calculation of the nonbonded interactions. For each mutated residue, the rotamer producing the lowest nonbonded energy was chosen, and a short optimization run restraining all non-H atoms to their initial coordinates allowed readjustment of covalent bonds and van der Waals contacts without changing the overall conformation of the protein.

Molecular modeling of nimesulide and conformational search

The three-dimensional structure of nimesulide has been determined by X-ray crystallography [27] and is deposited in the Cambridge Structural Database [28] (ref. WINWUL). In order to obtain an accurate representation of the electrostatic charge distribution, the molecular electrostatic potential (MEP) of nimesulide was calculated ab initio following full geometry optimization using the 6–31G* basis set [30]. Partial atomic charges were then derived by fitting the MEP to a monopole-monopole expression [31], and consistent bonded and non-bonded AMBER parameters [31] were obtained (Table 1).

The phase space for nimesulide was sampled by using a combination of quenched molecular dynamics and energy minimization techniques. The X-ray conformation was heated from 6 K to 600 $\pm$ 10 K in 10 ps using classical molecular dynamics and a time step of

Table 1. AMBER parameters and charges for nimesulide

Atom	Type	Charge	Atom	Type	Charge
H1	H4	0.2301	C18	CA	−0.2133
C2	CA	−0.2068	H19	H4	0.1609
C3	CA	−0.3012	C20	CA	−0.0621
H4	H4	0.2301	H21	H4	0.1503
C5	C	0.1183	C22	CA	−0.3846
N6	NO	0.8429	H23	H4	0.2027
O7	ON	−0.4937	C24	CA	0.2595
O8	ON	−0.4923	N25	NX	−0.6642
C9	CA	−0.4551	H26	H	0.3876
H10	H4	0.2613	S27	SX	1.2724
C11	C	0.3424	O28	O2	−0.6042
O12	OS	−0.4756	O29	O2	−0.5976
C13	C	0.5541	C30	CT	−0.5414
C14	CA	−0.3595	H31	HC	0.1698
H15	H4	0.2025	H32	HC	0.1805
C16	CA	−0.0758	H33	HC	0.2090
H17	H4	0.1527			

Table 1. (continued)

Bond	K_r (kcal mol^{-1} A^{-2})	r_{eq} (Å)
SX-CT	227.0	1.69
SX-O2	553.0	1.40
NX-SX	230.0	1.64
NX-H	434.0	1.00

Angle	K_θ (kcal mol^{-1} rad^{-2})	θ_{eq}
C-CA-C	63.0	120.0
C-CA-H4	35.0	120.0
SX-CT-HC	50.0	109.2
H-NX-SX	35.0	115.0
NX-SX-CT	50.0	105.0
NX-SX-O2	50.0	104.8
CA-NX-SX	50.0	129.8
CA-NX-H	38.0	115.2
CA-CA-NX	70.0	125.3
CA-C-OS	70.0	119.0
CA-C-NO	70.0	119.0
ON-NO-ON	90.0	123.5
C-NO-ON	50.0	118.2
C-CA-NX	70.0	115.6
C-OS-C	60.0	120.8
O2-SX-CT	80.0	108.0
O2-SX-O2	80.0	121.1
OS-C-CA	70.0	119.0

Dihedral angle	idivf	$V_n/2$ (kcal mol^{-1})	γ (deg)	n
CA-NX-SX-O2	1	0.25	0.0	−3
CA-NX-SX-O2	1	1.20	0.0	2
H-NX-SX-O2	1	0.25	0.0	−3
H-NX-SX-O2	1	1.20	0.0	2
H-NX-SX-CT	1	0.0	0.0	2
CA-NX-SX-CT	1	0.0	0.0	2
X-CA-NX-SX	2	4.23	180.0	2
X-SX-CT-X	9	0.9	0.0	3
C-OS-C-CA	1	1.8	180.0	2
CA-C-NO-ON	1	2.15	180.0	2

Improper torsional angle	$V_n/2$ (kcal mol^{-1})	γ (deg)	n
X-CA-C-OS	1.1	180	2
CA-CA-C-NO	10.5	180	2
CA-C-CA-NX	0.5	180	2

Van der Waals	R∗ (Å)	ϵ (kcal mol^{-1})
NX	1.824	0.17
SX	2.000	0.25

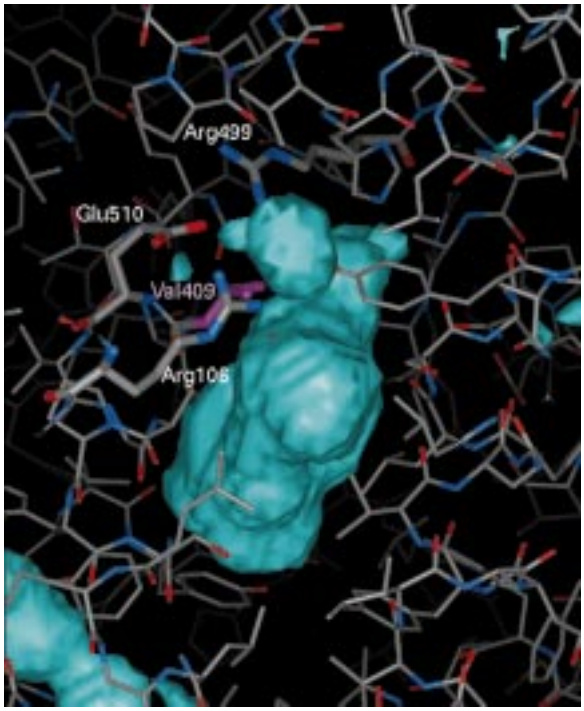

Figure 3. MEP of the cyclooxygenase active site of hPGHS-2 (contoured in blue at +3 kcal/mol). Note that no solution of continuity is apparent between the substrate binding channel and the adjacent pocket that is occupied by nimesulide and other selective COX-2 inhibitors.

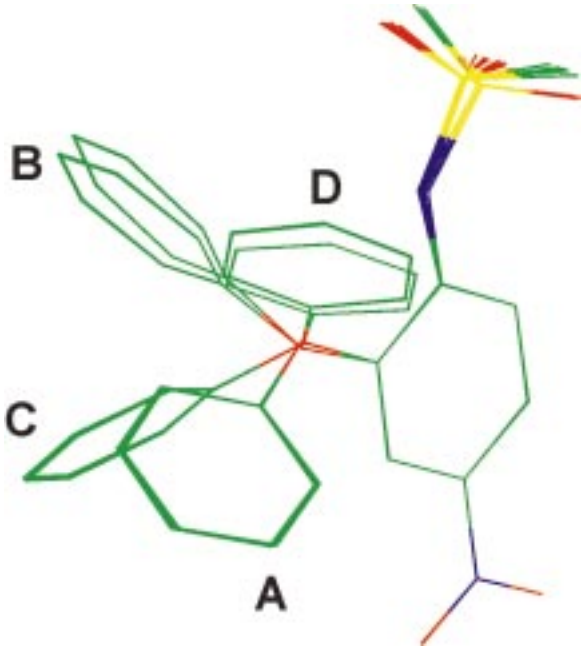

Figure 4. Conformational families found for nimesulide after the high temperature molecular dynamics simulations. Hydrogen atoms are not shown for clarity. The molecules have been superimposed using the nitrophenyl ring as a common frame of reference. Conformers A and B, which belong to two low-energy subsets, correspond to docked conformations A and B in Figure 5 and Table 2.

0.5 fs. After a further 20 ps of equilibration, it was slowly cooled down back to the initial temperature and energy minimized by using 100 steps of the steepest descent method and then switching over to conjugate gradient until the root-mean-square gradient was less than 0.01 kcal mol^{-1} $Å^{-1}$. The resulting structure was subjected to the same simulated annealing protocol, and the whole procedure was repeated 50 times. One member from each resulting conformational family was then selected to be used as input for the rigid ligand docking methods.

Docking methods

Both rigid and flexible ligand docking methods were employed, and the selective inhibitor SC-558 (Figure 2), as found in its complex with mouse COX-2 [15], was used as a control of program performance.

With the aid of program GRID [32], a cubic lattice of points spaced at 0.3 Å was established throughout and around the cyclooxygenase active site of hPGHS-2 in order to search for regions that could give rise to favorable interactions with the functional groups present in nimesulide. At each lattice point the interactions between the protein and aromatic carbon (C1=), ether oxygen (OC2), sulfo oxygen (OS), nitro oxygen (ON), and amino nitrogen (N1:) probes were calculated. The resulting grids were contoured at appropriate energy levels and graphically displayed to aid in the visualization of complementarity regions. The same space was gridded at 1.0 Å and extra affinity maps were generated using H, water, and hydrophobic probes in order for subroutine GROUP to perform a rigid body docking with each of the selected conformers.

For the DOCK [33] studies, a molecular surface representation of the binding site was obtained by using the MS program [34] and a spherical probe of 1.4 Å radius. The surface points and their associated normals were used by program SPHGEN [35] to fill the active site with spheres of varying sizes (between 1.4 and 4 Å radii), the total volume of which provided a geometric description of the volume available to the ligands. The resulting cluster containing 38 spheres was enclosed in a $23 \times 16 \times 19$ $Å^3$ box which was gridded with a spacing of 0.25 Å so that each point

in the cubic lattice could be evaluated as making favorable or unfavorable contacts with receptor atoms (*contact scoring*) or used to store steric and electrostatic information of the receptor atoms within a 15.0 Å cut-off of the point (*force field scoring*). Polar and nonpolar contact limits for filtering were 2.3 and 2.8 Å. Each of the selected nimesulide conformers identified in the previous search was then input to DOCK in order to examine their binding potential and their preferred binding orientations.

The Monte Carlo simulated annealing technique implemented in AutoDock [36] was also used to generate different nimesulide conformers within the binding site by randomly changing torsion angles and overall orientation of the molecule. Rapid intra- and intermolecular energy evaluation of each configuration was achieved by having the receptor's atomic affinity potentials for carbon, oxygen, nitrogen, sulfur, and hydrogen atoms precalculated in a three-dimensional grid [32] with a spacing of 0.25 Å.

Energy refinement of the complexes and molecular dynamics simulations

The resulting complexes were gradually refined in AMBER using a cutoff of 10.0 Å. Since the binding site is completely buried within the protein, and only a reduced model of the whole protein was employed, no explicit water molecules were included but a distance-dependent dielectric constant ($\epsilon = 4r_{ij}$) was used to dampen the electrostatic interactions. First, only the nimesulide atoms were allowed to move; then, the amino acid side chains were also included in the energy minimization, and finally the whole complex was energy minimized although the protein backbone atoms were restrained to their initial positions with a force constant of 2 kcal mol^{-1} Å^{-2}. In each case, 100 steps of steepest descent were followed by conjugate gradient until the root-mean-square value of the potential energy gradient was below 0.01 kcal mol^{-1} Å^{-1}. The final coordinate set was used as input for the subsequent molecular dynamics simulation under the same dielectric and restraining conditions. In a 5-ps heating phase, the temperature was raised from 0.2 to 298 K, and the velocities were reassigned at each new temperature according to a Maxwell-Boltzmann distribution. A 1-ns trajectory was then simulated at 298 K employing a time step of 2 fs. The SHAKE algorithm was used to constrain all bonds involving hydrogens to their equilibrium values. The list of nonbonded pairs was updated every 25 steps and coordinates were saved every 2 ps for further analysis.

Continuum electrostatics

Finite difference solutions to the linearized Poisson–Boltzmann equation [37], as implemented in the DelPhi module of Insight-II [25], were used to calculate electrostatic potentials and energies. Cubic grids with a resolution of 0.5 Å were centered on the molecular systems considered, and the charges were distributed onto the grid points. Solvent-accessible surfaces, calculated with a spherical probe of 1.4 Å radius, defined the solute boundaries, and a minimum separation of 11 Å was left between any solute atom and the borders of the box. The potentials at the grid points delimiting the box were calculated analytically by treating each charge atom as a Debye–Hückel sphere. The accuracy of the calculated electrostatic potentials was subsequently improved by defining a smaller grid with a lower resolution (0.25 Å spacing) and using boundary potentials linearly interpolated from those calculated in the previous run. The interior of the protein, the ligands and the complexes was considered a low dielectric medium ($\epsilon = 4$) whereas the surrounding solvent was treated as a high dielectric medium ($\epsilon = 80$).

The change in electrostatic free energy of nimesulide upon binding (ΔGele) was computed by running 3 consecutive calculations: one for all the atoms in the complex (Gele^{LR}), one for the ligand atoms alone (Gele^{L}), and a third one for the receptor atoms alone (Gele^{R}). By using the same grid definition in the three calculations, the artifactual grid energy cancels out and the electrostatic contribution to the binding free energy can be expressed as the difference $\Delta\text{Gele} = \text{Gele}^{LR} - (\text{Gele}^{L} + \text{Gele}^{R})$ [38, 39].

Results

Description of the binding site in the modelled human enzyme

Mainly as a result of the replacement of Ile-523 with a valine (Figure 1), the volume accessible to both substrates and inhibitors in the COX active site increases in PGHS-2 relative to PGHS-1. The shorter side chain of Val-509 allows this binding site to be extended in PGHS-2 past the bottom of the substrate binding channel up into a neighboring pocket that leads directly to

the solvent. The enlarged volume of the binding site is readily apparent from both the clusters of spheres generated by DOCK and the energy maps calculated by GRID with a methyl probe (data not shown). In addition to the increase in size, the MEP calculated with DelPhi also reveals that the positive potential in the vicinity of Arg-106 extends into this side pocket in which an arginine (Arg-499) occupies the position of His-513 in PGHS-1 (Figure 3).

Conformational study

The high temperature molecular dynamics procedure allowed nimesulide to cross energy barriers in the multidimensional conformational space and provided us with a sample of conformations and their potential energies. It was revealed that the range of conformations available for nimesulide is rather limited. There are four major conformational families that differ in the relative orientation of the aromatic rings, and several subfamilies that arise from rotation about the NH-SO_2 bond (Figure 4). The energy differences among them were sufficiently small ($<$10 kcal mol^{-1}) as to consider them all as candidates for the bound conformation.

Docking

Test docking calculations using the COX-2 selective inhibitor SC-558 [15] showed that the three methods – GRID, DOCK and AutoDock – could reproduce the experimental binding mode of this ligand (root-mean-square deviations for all heavy atoms below 1.0 Å). For nimesulide, the three docking methods agreed on a binding mode that makes use of the adjacent pocket accessible from the bottom of the substrate channel but two different binding orientations were obtained. The orientation favored by AutoDock (orientation A) placed the methanesulfonanilide moiety in the side pocket, leaving the nitro group close to Arg-106 in the substrate channel (Figure 5A). The DOCK program assigned a better force-field score to an alternate orientation (orientation B), which was also found by AutoDock as the second best, that places the sulfo group in the vicinity of Arg-106 and the nitro group in the side pocket close to Arg-499 (Figure 5B). In both cases, the phenoxy ring occupies a position comparable to that of the bromophenyl ring of SC-558 (Figure 2) or the distal phenyl ring of flurbiprofen in the respective crystallographic complexes of these drugs with PGHS-2 [15], that is, close and perpendicular to the aromatic ring of the catalytic tyrosine (Tyr-371) and in van der Waals contact with Leu-338. Both orientations, which differ by 180° in the value of torsional angle $\phi_{C24-C11-O12-C13}$ (Figure 4), were also found by the GRID program, depending on the conformer studied. By comparing the DOCK and AutoDock results, for which energy partitioning of the scoring function is possible, the differences in interaction energy between orientations A and B arise mainly from electrostatic and van der Waals contributions emanating from the nitro and the methyl group in the two different enzyme environments. In the AMBER-refined complexes, the overall intermolecular interaction energy is very similar given that a better electrostatic term in complex A is compensated by an improved van der Waals contribution in complex B. As regards the intramolecular energy of nimesulide, the drug is in a comparable low-energy conformation in both orientations.

Molecular dynamics simulations and energy analysis

To take into account protein flexibility, which may be a functional component of ligand binding [15], as well as the possibility of conformational changes analogous to those reported for RS-57067 [14], the behavior of both complexes was studied in a dynamic context and the van der Waals and electrostatic components of the interaction energy were monitored (Figure 6). Both complexes remained stable during the whole trajectory and yielded almost equivalent overall interaction energies. Orientation A, which places the sulfonamide group close to Arg-499 (and is therefore similar to the orientation observed in the complex of mouse PGHS-2 with SC-558) consistently gives rise to a slightly more favorable electrostatic interaction whereas the van der Waals interaction is slightly better when this group is close to Arg-106 (orientation B). In order to evaluate the relative contributions of the different residues to complex stabilization the 100 structures collected from the last 200 ps of the simulations were averaged and energy-minimized, and the interaction energy between nimesulide and the binding site was decomposed on a residue basis using the ANAL module of AMBER (Table 2). It can be seen that the major contributors to the binding energy are Val-509 and Leu-338, and that the relative importance of Arg-499 and Arg-106 depends on the orientation considered.

The continuum electrostatics calculations on the same complexes, which take into account the cost of desolvation, afforded similar results (around 1 kcal mol^{-1} more favorable electrostatic binding en-

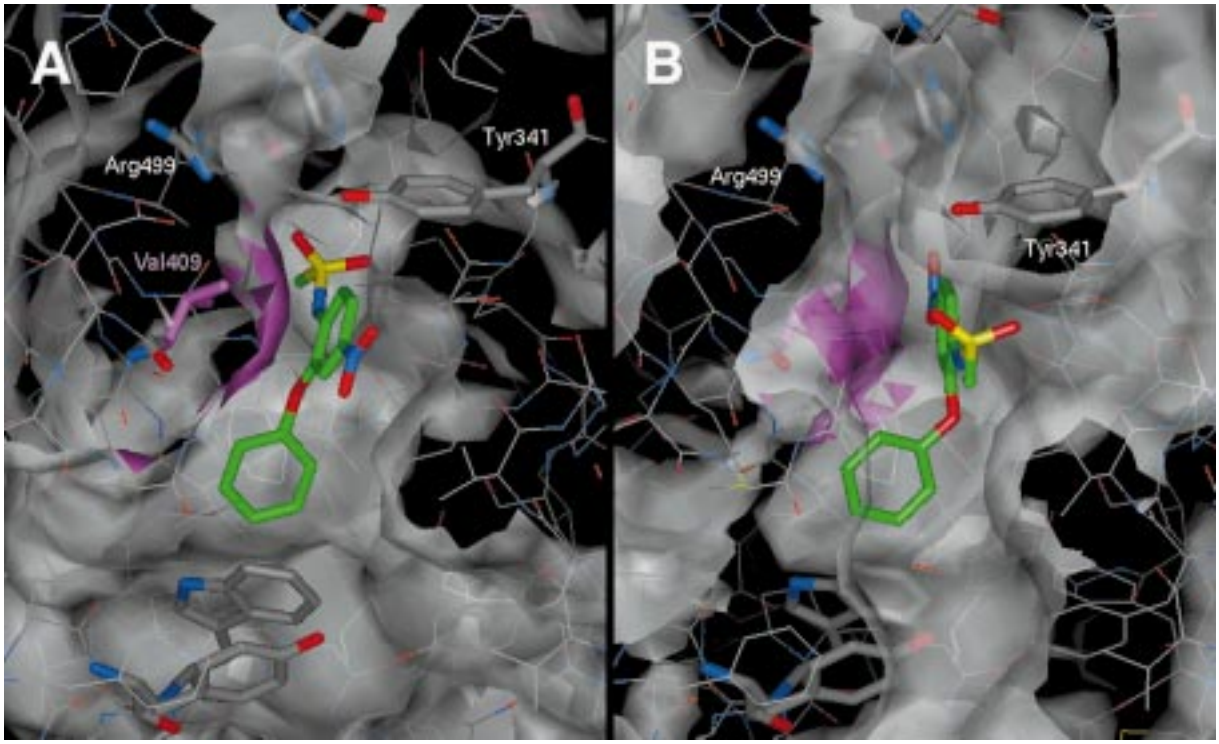

Figure 5. Nimesulide (carbon atoms colored in green) bound in the cyclooxygenase active site of hPGHS-2 (carbon atoms colored in grey). A semi-transparent pseudo-Connolly surface is used to highlight the volume available for the ligands. The crucial valine that allows access to the side pocket at the bottom of the substrate binding channel is labeled and colored in pink. The two orientations found for nimesulide are shown (A and B), and residues relevant to the discussion are displayed as thick sticks.

Table 2. Residue-based energy decomposition of the interaction energy between nimesulide and the COX active site of hPGHS-2 in the two orientations studied

Protein residue	Orientation A			Orientation B		
	van der Waals	electrostatic	Total	van der Waals	electrostatic	Total
His75	−2.1	−0.6	−2.7	−1.5	−0.4	−1.9
Arg106	−1.8	−0.6	−2.4	−1.5	−2.8	−4.3
Val335	−2.5	0.0	−2.5	−2.9	0.2	−2.7
Leu338	−4.5	0.1	−4.4	−5.2	−0.1	−5.3
Ser339	−3.9	0.3	−3.6	−4.5	−0.1	−4.6
Tyr341	−2.6	−0.1	−2.7	−3.8	0.3	−3.5
Arg499	−2.6	−2.0	−4.6	−0.9	−0.3	−1.2
Phe504	−4.8	0.2	−4.6	−4.4	0.1	−4.3
Val509	−5.7	−0.1	−5.8	−5.7	0.0	−5.7
Ala513	−2.2	−0.0	−2.2	−2.2	0.0	−2.2

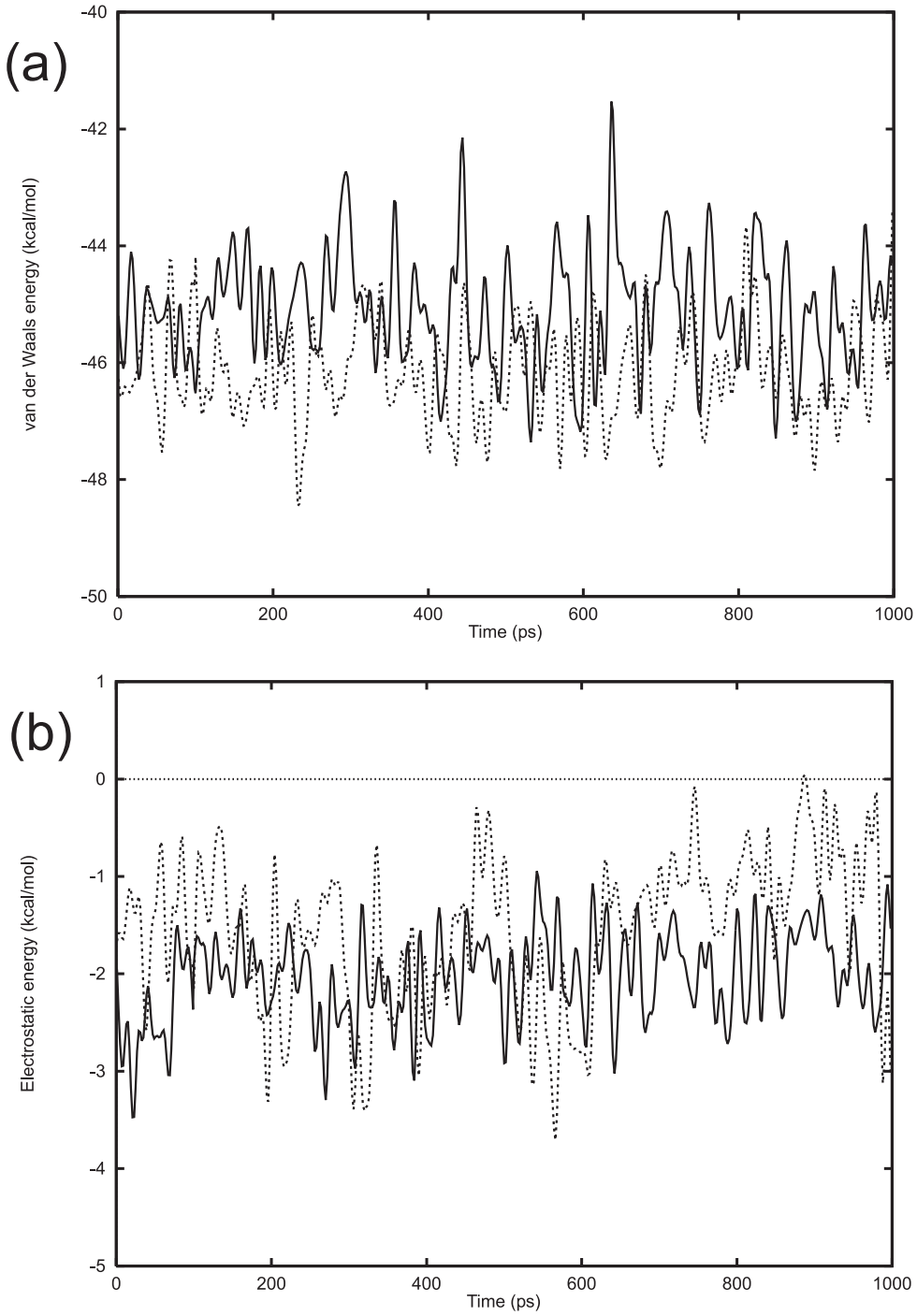

Figure 6. (a) van der Waals and (b) electrostatic interaction energies between nimesulide and COX-2 monitored during the 1-ns molecular dynamics simulations. The data were smoothed after filtering high-frequency noise by 'moving window' averaging (*boxcar smoothing*) using a window width of 10 ps (5 sets of values) [62]. Solid and broken lines denote complexes A and B, respectively.

ergy for orientation A). This is not surprising given that in both orientations the ligand is completely buried and occupies the same volume within the binding site so that desolvation equally affects both complexes.

Discussion

The alignment of the primary sequences of PGHS-1 and PGHS-2 from different sources demonstrates that the majority of the changes between the two isoforms occur at the N-terminal region forming the amphipathic helices that presumably constitute the membrane-binding domain, and at the C-terminal tail. The COX active sites of PGHS-1 and PGHS-2, on the other hand, are very similar, the only differences in the first shell of residues lining the cavity being an Ile→Val and a His→Arg substitution (Figure 1).

The structural studies on murine PGHS-2 have shown that the conformation of the free enzyme in the crystal is very similar to that of the enzyme in the crystallographic complexes with both selective and non-selective inhibitors [15]. On the other hand, the residues making up the COX active site in mouse and human PGHS-2 are identical (Figure 1), which supports the view that both binding sites must also be very similar [15] and lends credence to the present model. The reported flexible nature of the human COX-2 binding site [14] was taken into account in our restrained molecular dynamics simulations, which were carried out for the two alternate orientations of nimesulide suggested by the automated docking programs.

Both binding modes are chemically reasonable, yield very similar interaction energies with the enzyme (Figure 6), and are in agreement with the fundamental role played by the side chain of Val-509. Attempts to discriminate between the two models are hampered by the rather limited structure-activity data for nimesulide but both complexes will now be examined in the light of the experimental evidence available for this drug and other structurally and pharmacologically related compounds, such as NS-398 [40, 41] and flosulide [42] (Figure 2).

For nimesulide and related compounds, inhibition of COX-1 activity is competitive and rapidly reversible but inhibition of COX-2 is characterized by being time-dependent [4, 43–46] presumably due to a structural transition. The molecular basis of COX-2 inhibition by isoform-selective agents has been probed by site-directed mutagenesis experiments on both COX-1 and COX-2. Several mutations at the mouth of the active site of COX-2 did not lead to changes in the selectivity of COX-2 inhibitors [47]. On the contrary, two residues that are not conserved between the two isoforms and impinge on selectivity are Arg-499 and Val-509 of PGHS-2, which are His-513 and Ile-523 in PGHS-1, respectively (Figure 1). Thus, the single amino acid change of Val at position 509 of PGHS-2 to Ile results in a loss of sensitivity to inhibition by nimesulide, NS-398 and other related COX-2 selective inhibitors such as 5-bromo-2-(4-fluorophenyl)-3-(4-methylsulfonyl)thiophene (DuP697) while inhibition by other non-selective NSAIDs such as indomethacin remains unaffected [47]. Similarly, V509A, V509K and V509E PGHS-2 mutants, like recombinant human PGHS-1, show reversible but not time-dependent inhibition with nimesulide [45].

The role of Val-509 as an essential determinant in the differential interaction of PGHS-2 with selective and non-selective inhibitors is also patent from experiments with the Ile-523→Val PGHS-1 mutant, which displays increased sensitivity to various COX-2 selective inhibitors, including NS-398 [46]. Interestingly, this sensitivity is not altered in a His513→Arg PGHS-1 mutant but the simultaneous occurrence of both mutations results in increased inhibition by NS-398 relative to the single Ile523→Val mutant, and also in time-dependent inhibition. This highlights the importance of a second positively charged residue in the COX-2 binding site in addition to Arg-106 for ionic interactions with substrates and nimesulide-like inhibitors, and is in accordance with our models (Table 2). Nevertheless, although both mutations appear to be necessary to change the rapidly reversible mechanism of PGHS-1 inhibition to the time-dependent mechanism characteristic of PGHS-2 inactivation, not all the properties of the active site of PGHS-2 are restored by these two mutations. In fact, the double mutant does not synthesize any appreciable amount of 15-HETE when treated with 100 μM aspirin (ASA), in contrast with ASA-inhibited PGHS-2. This may be an indication that additional amino acid changes may be involved as, for example, another Ile→Val substitution at position 434 (PGHS-1 numbering), which has been proposed to facilitate access to the side pocket [15].

Acetylation of Ser-516 by ASA or mutation of this residue to methionine, on the other hand, does not greatly affect the binding and inhibitory properties of NS-398 or DuP697, as opposed to meclofenamic acid

or diclofenac, which are potent inhibitors of PGHS-2 but do not inhibit either ASA-PGHS-2 or the S516M mutant enzyme [48]. In accordance with these mutagenesis data, this residue does not appear to be directly involved in the binding of nimesulide as either the nitro or the sulfo oxygens are 5–7 Å from the hydroxyl group of Ser-516.

Biochemical [49] and structural evidence [11–15] attests to the importance of Arg-120 in PGHS-1 (or Arg-106 in PGHS-2) for interacting both with the carboxylic acid group of arachidonic acid and with the free carboxylic acid moiety of several NSAIDs. The contribution of this positively charged residue to substrate binding in PGHS-2, however, is less than that of the equivalent Arg-120 in PGHS-1, as shown by the effects on enzymatic activity of replacing this arginine residue by glutamic acid (increases in K_m of $\sim$30 vs. $\sim$100 [50] or more [51], respectively). This difference may be related to the increased positive electrostatic potential brought about by the presence of Arg-499 in the accessible side pocket nearby (Figure 3). As regards the binding of inhibitors, the effect of such a charge reversal mutation depends on the class of inhibitor considered. Thus, the inhibition of hPGHS-2(R106E) by DuP697 is not affected but the same Arg106→Glu mutation results in 600- and 1000-fold decreases in potency for flosulide and NS-398. This loss of effect is due to a difference in the kinetics of inhibition, with these two drugs displaying time-dependent inhibition of hPGHS-2 but time-independent inhibition of hPGHS-2(R106E) [50]. In agreement with the involvement of this Arg in the tight binding of this class of inhibitors, the models we propose for nimesulide give rise to rather strong electrostatic interactions with both Arg residues in any of the two orientations considered (Table 2).

The X-ray crystal studies have consistently shown Arg-120 in PGHS-1 to be engaged in a salt bridge with the carboxylic group of Glu-524 [11–13], and these two residues, together with Tyr-355, to participate in a hydrogen bond network at the bottom of the COX active site in which ligand atoms are also involved. Tyr-355 is a determinant of the stereospecificity of PGHS-1 toward inhibitors of the 2-phenylpropionic acid class [51] but Glu-524 does not appear to be importantly involved in catalysis or substrate binding, as suggested by results obtained with E524D, E524Q, and E524K PGHS-1 mutants [51]. The corresponding residues in PGHS-2 also participate in a similar hydrogen bond network in the free enzyme and in the complexes with non-selective inhibitors [15] but in some of the complexes with COX-2 selective inhibitors the salt bridge between Arg-106 and Glu-510 is disrupted because the side chain of this latter residue is reoriented so as to form a salt bridge with Arg-499 on the other side of the extended binding site. This is observed in the complexes of mouse PGHS-2 with SC-558 and hPGHS-2 with RS-57067, an analog of the non-selective NSAID zomepirac in which replacement of the carboxylic group with a pyridazinone ring leads to preferential inhibition of PGHS-2 [14, 52]. By contrast, in the complex of hPGHS-2 with the related analog RS-104897 (Figure 2), this reorientation is not observed, and the acylsulfonamide group of this drug interacts, in a manner similar to the carboxylic group of flurbiprofen or indomethacin [12, 15], not only with Arg-106 but also with Tyr-341 [14], a residue that is known to be involved in the molecular mechanism of time-dependent inhibition of PGHS-2 [52]. In our models with nimesulide, dual interactions with Arg-106 and Tyr-341 are also observed but, depending on the orientation of the drug in the binding site, it is either the nitro or the sulfonamide group that interacts with the side chain of either Arg-106 or Arg-499 (Figure 5). During the molecular dynamics simulations, we find that in the complexes of hPGHS-2 with nimesulide, in addition to the reported hydrogen bond network in the COX active site, there appears to be an interesting and dynamic network of alternating salt bridges involving a number of residue pairs: Arg106-Glu510, Glu510-Arg499, Arg499-Glu506, Glu506-Arg453, and Arg453-Glu496. This dynamic picture complements the static X-ray data and deserves further study.

The sulfonamide NH of nimesulide does not appear to make any direct contacts with the protein. Its major role appears to be in limiting the conformational flexibility of the phenoxy moiety and in enforcing the co-planarity of the sulfonamide group with respect to the nitrophenyl ring. Methylation of the equivalent nitrogen in the related flosulide (Figure 2) has been shown to result in complete loss of in vitro COX-2 inhibitory activity [42]. In the light of the present docking experiments, this is not surprising given that *N*-methylation would bring about a conformational change in the ligand incompatible with the strict geometric requirements of this binding site (Figure 5). It is also known that the nitro group of nimesulide can not be replaced with a cyano group or a tetrazol ring [53], and that replacement by a hydroxyl (as in the main metabolite of nimesulide) is accompanied by a

20-fold loss of activity in whole blood assays in vitro [20].

An indication that the side chain of valine is more important for nimesulide in order to form a tight complex with PGHS-2 than it is for other related inhibitors comes from experiments that show that the V509A PGHS-2 mutant is inhibited in a time-dependent fashion by NS-398 and DuP697 but not by nimesulide [44]. From the values shown in Table 2 it is apparent that the interaction of the drug with this residue is important but very similar for both orientations. The complementarity with the GRID map generated with a methyl probe is somewhat better for orientation A, but the difference is small (data not shown). In the complex of mouse PGHS-2 with SC-558, the more polar sulfonamide group of the drug interacts with the side chains of Arg-499 and Gln-178 in the pocket adjacent to the substrate binding channel that non-selective inhibitors do not occupy [15] while the trifluoromethyl group is located close to Arg-106. No group in nimesulide appears to interact directly with Gln-178 but a hydrogen bonding interaction is possible with His-75 (Figure 5).

Inspection of ligand-receptor complexes deposited in the PDB with ReLiBase tools [54] reveals a similar protein environment for nitro and sulfo groups of ligands and a similar tendency of these moieties to interact with the guanidinium group of arginine residues. In accordance with this, the GRID maps generated for ON and OS probes are only subtly different and match the positions of both functional groups in the bound conformations of nimesulide so that both binding modes remain feasible. In this respect, it is of interest to note that multiple modes of binding have been suggested for the interaction between diarylheterocyclic compounds and PGHS-2 [15] and also that reversal of the functionalities in some substituted 1,5-diphenylpyrazoles brings about striking changes in potency and selectivity [9].

Conclusions

Nimesulide has been on the market for a number of years as an antiinflammatory agent [1, 21] and has recently been shown to inhibit PGHS-2 preferentially over PGHS-1 in man [19]. Interest in this drug is warranted not only by its gastrointestinal safety profile as a rather selective COX-2 NSAID [18] but also in the light of recent experiments that show it to exert a suppressive effect on azoxymethane-induced colon carcinogenesis in mice [55] and to prevent urinary bladder carcinomas in rats [56]. Nevertheless, no structural details of its interaction with COX enzymes are available except for two theoretical studies involving wild-type and mutant ovine PGHS-1 [57, 58].

Our simulations show that nimesulide is a relatively rigid ligand, with a limited repertoire of conformations (Figure 4), all of which have been considered in the present docking calculations. The three different automated docking methods used provided us with two possible orientations for nimesulide in the cyclooxygenase active site of hPGHS-2 which can account for the pharmacological profile of this agent as a COX-2 selective inhibitor. Nimesulide is proposed to bind PGHS-2 at the bottom of the substrate channel where it gains access to an adjacent pocket, the entrance to which is more restricted in COX-1 as a result of the presence of an isoleucine at position 523 in place of a valine (Figure 5). Two possible orientations are found depending on whether the nitrophenyl or the sulfoanilide ring gets sandwiched in the hydrophobic environment between the side chain of this valine (Val-499) and the C_α and C_β atoms of Ser-339.

Molecular dynamics simulations and energy analysis of the two complexes were carried out in an attempt to distinguish between the two alternate binding modes. In one orientation the side chain of Arg-106 interacts with the nitro group whereas in the alternate one it is the sulfonamide group that interacts with this positively charged residue. Conversely, Arg-499 and His-75 can establish hydrogen bonding interactions with either the sulfonamide or the nitro group of nimesulide in the side pocket of this enlarged binding site. In both cases, the unsubstituted phenoxy ring lies in close proximity to Leu-338 and the catalytic tyrosine residue thus blocking the approach of the arachidonic acid substrate. On the basis of our binding energy calculations, we cannot discriminate between these two binding modes, so the possibility that nimesulide binds in the COX active site of hPGHS-2 in both orientations can not be ruled out. Although use could have been made of free energy perturbation techniques [59] or the linear response method [60] to calculate the absolute binding free energies of nimesulide in the two orientations, these computer-intensive approaches are beyond the scope of the present investigation. Clearly, the details of the interaction will be more completely elucidated when the crystal structure of the complex is solved.

Acknowledgements

We thank Prof. Irwin Kuntz (Molecular Design Institute), Dr Peter J. Goodford (Molecular Discovery Ltd.), and Dr Garret Morris (The Scripps Research Institute) for provision of the programs DOCK, GRID and AutoDock, respectively. This research has been financed in part by Alter S.A. (Madrid, Spain) and Helsinn Healthcare (Lugano, Switzerland). C.P. is the recipient of a fellowship from the Spanish Ministerio de Educación y Cultura.

References

1. Vane, J.R., Bakhie, Y.S. and Botting, R.M., Annu. Rev. Pharmacol. Toxicol., 38 (1998) 97.
2. Spencer, A.G., Woods, J.W., Arakawa, T., Singer I.I. and Smith, W.L., J. Biol. Chem., 273 (1998) 9886.
3. Meade, E.A., Smith, W.L. and DeWitt, D.L., J. Biol. Chem., 268 (1993) 6610.
4. Laneuville, O., Breuer, D.K., Dewitt, D.L., Hia, T., Funk, C.D. and Smith, W.L., J. Pharmacol. Exp. Ther., 271 (1994) 927.
5. Riendeau, D., Charieson, S., Cromlish, W., Mancini, J.A., Wong, E. and Guay, J., Can. J. Physiol. Pharmacol., 75 (1997) 1088.
6. Copeland, R.A., Williams, J.M., Giannaras, J., Nurnberg, S., Covington, M., Pinto, D., Pick, S. and Trzaskos, J.M., Proc. Natl. Acad. Sci. USA, 91 (1994) 91, 11202.
7. Khanna, I.K., Weier, R.M., Yu, Y., Xu, X.D., Koszyk, F.J., Collins, P.W., Koboldt, C.M., Veenhuizen, A.W., Perkins, W.E., Casier, J.J., Masferrer, J.L., Zhang, Y.Y., Gregory, S.A., Seibert, K. and Isakson, P.C., J. Med. Chem., 40 (1997) 1634.
8. Khanna, I.K., Weier, R.M., Yu, Y., Collins, P.W., Miyashiro, J.M., Koboldt, C.M., Veenhuizen, A.W., Currie, J.L., Seibert, K. and Isakson, P.C., J. Med. Chem., 40 (1997) 1619.
9. Penning, T.D., Talley, J.J., Bertenshaw, S.R., Carter, J.S., Collins, P.W., Docter, S., Graneto, M.J., Lee, L.F., Malecha, J.W., Miyashiro, J.M., Rogers, R.S., Rogier, D.J., Yu, S.S., Anderson, G.D., Burton, E.G., Cogburn, J.N., Gregory, S.A., Koboldt, C.M., Perkins, W.E., Seibert, K., Veenhuizen, A.W., Zhang, Y.Y. and Isakson, P.C., J. Med. Chem., 40 (1997) 1347.
10. Kalgutkar, A.S., Kozak, K.R., Crews, B.C., Hochgesang, G.P. Jr. and Marnett, L.J., J. Med. Chem., 41 (1998) 4800.
11. Picot, D., Loll, P.J. and Garavito, R.M., Nature, 367 (1994) 243.
12. Loll, P.J., Picot, D., Ekabo, O. and Garavito, R.M., Biochemistry, 35 (1996) 7330.
13. Loll, P.J., Picot, D. and Garavito, R.M., Nat. Struct. Biol., 2 (1995) 637.
14. Luong, C., Miller, A., Barnett, J., Chow, J., Ramesha, C. and Browner, M.F., Nat. Struct. Biol., 3 (1996) 927.
15. Kurumbail, R.G., Stevens, A.M., Gierse, J.K., McDonald, J.J., Stegeman, R.A., Pak, J.Y., Gildehaus, D., Miyashiro, J.M., Penning, T.D., Seibert, K., Isakson, P.C. and Stailings, W.C., Nature, 384 (1996) 644.
16. Marnett, L.J. and Kaigutkar, A.S., Curr. Opin. Chem. Biol., 4 (1998) 482.
17. Swingle, K.F., Moore, G.G.I. and Grant, T.J., Arch. Int. Pharmacodyn., 221 (1976) 132.
18. Famaey, J.P., Inflamm. Res., 46 (1997) 437.
19. Cullen, L., Kelly, L., Connor, S.O. and Fitzgerald, D.J., J. Pharmacol. Exp. Ther., 287 (1998) 578.
20. Panara, M.R., Padovano, R., Sciuii, M.G., Santini, G., Renda, G., Rotondo, M.T., Pace, A., Patrono, C. and Patrignani, P., Clin. Pharmacol. Ther., 63 (1998) 672.
21. Hardman, J.G., Gilman, A.G. and Limbird, L.E. (Eds.) Goodman & Gilman's The Pharmacological Basis of Therapeutics, 9th ed., McGraw-Hill, New York, NY, 1996.
22. Vigdahl, R.L. and Tukey, R.H., Biochem. Pharmacol., 126 (1977) 307.
23. García-Nieto, R., Pérez, C., Checa, A. and Gago, F., 11th EULAR Symposium, Geneva, Switzerland, September 5–8, 1998.
24. Bernstein, F.C., Koetzle, T.F., Williams, G.J.B., Meyer, E.F. Jr., Brice, M.D., Rodgers, J.R., Kennard, O., Shimanouchi, T. and Tasumi, M., J. Mol. Biol., 112 (1977) 535.
25. Insight II, version 97.2, 1998. Molecular Simulations Inc., San Diego, CA.
26. Pearlman, D.A., Case, D.A., Caldwell, J., Ross, W.S., Cheatham, T.E., Ferguson, D.M., Seibel, G.L., Singh, U.C., Weiner, P. and Kollman, P.A., AMBER version 4.1 (1995), Department of Pharmaceutical Chemistry, University of California, San Francisco, CA.
27. Dupont, L., Pirotte, B., Masereel, B., Delarge, J. and Geczy, J., Acta Crystallogr., C51 (1995) 507.
28. Allen, F.H., Bellard, S., Brice, M.D., Cartwright, B.A., Doubleday, A., Higgs, H., Hummelink, T., Hummelink-Peters, B.G., Kennard, O., Motherwell, W.D.S., Rodgers, J.D. and Watson, D.G., Acta Crystallogr., B35 (1979) 2331.
29. Gaussian 94, Revision E.1, Frisch, M.J., Trucks, G.W., Schlegel, H.B., Gill, P.M.W., Johnson, B.G., Robb, M.A., Cheeseman, J.R., Keith, T., Petersson, G.A., Montgomery, J.A., Raghavachari, K., Al-Laham, M.A., Zakrzewski, V.G., Ortiz, J.V., Foresman, J.B., Cioslowski, J., Stefanov, B.B., Nanayakkara, A., Challacombe, M., Peng, C.Y., Ayala, P.Y., Chen, W., Wong, M.W., Andres, J.L., Replogle, E.S., Gomperts, R., Martin, R.L., Fox, D.J., Binkley, J.S., Defrees, D.J., Baker, J., Stewart, J.P., Head-Gordon, M., Gonzalez, C. and Pople, J.A., Gaussian, Inc., Pittsburgh, PA, 1995.
30. Besler, B.H., Merz, K.M. and Kollman, P.A., J. Comput. Chem., 11 (1990) 431.
31. Cornell, W.D., Cieplak, P., Bayly, C.I., Gould, I.R., Merz, K.M., Ferguson, D.M., Spellmeyer, D.C., Fox, T., Caldwell, J.W. and Kollman, P.A., J. Am. Chem. Soc., 117 (1995) 5179.
32. GRIN, GRID, GRAB, and GROUP version 16.0, Molecular Discovery Ltd., 1998.
33. DOCK, version 3.5, Molecular Design Institute, University of California, San Francisco, CA, 1995.
34. Connolly, M.L., J. Appl. Crystallogr., 16 (1983) 548.
35. Kuntz, I.D., Blaney, J.M., Oatley, S.J., Langridge, R. and Ferrin, T.E., J. Mol. Biol., 161 (1982) 269.
36. AutoDock: Automated Docking of Flexible Ligands to Receptors, Version 2.4 (1996), Morris, G.M., Goodsell, D.S., Huey, R. and Olson, A.J., The Scripps Research Institute, La Jolla, CA.
37. Warwicker, J. and Watson H.C., J. Mol. Biol., 157 (1982) 671.
38. Honig, B. and Nicholls, A., Science, 268 (1995) 1144.
39. Checa, A., Ortiz, A.R., de Pascual-Teresa, B. and Gago, F., J. Med. Chem., 40 (1997) 4136.
40. Futaki, N., Takahashi, S., Yokoyama, M., Arai, I., Higuchi, S. and Otomo, S., Prostaglandins, 47 (1994) 55.
41. Harada, Y., Kawamura, M., Hatanaka, K., Saito, M., Ogino, M., Ohno, T., Ogino, K. and Yang, Q., Prostaglandins Other Lipid. Mediat., 55 (1998) 345.

42. Li, C.S., Black, W.C., Chan, C.C., Ford-Hutchinson, A.W., Gauthier, J.Y., Gordon, R., Guay, D., Kargman, S., Lau, C.K., Mancini, J., Ouimet, N., Roy, P., Vickers, P., Wong, E., Young, R.N., Zamboni, R. and Prasit, P., J. Med. Chem., 38 (1995) 4897.
43. Vago, T., Arzneimittelforschung, 45 (1995) 1096.
44. Ouellet, M. and Percival, M.D., Biochem J., 306 (1995) 247.
45. Guo, Q., Wang, L.H., Ruan, K.H. and Kulmacz, R.J., J. Biol. Chem., 271 (1996) 19134.
46. Wong, E., Bayly, C., Waterman, H.L., Riendeau, D. and Mancini, J.A., J. Biol. Chem., 272 (1997) 9280.
47. Gierse, J.K., McDonald, J.J., Hauser, S.D., Rangwala, S.H., Koboldt, C.M. and Seibert, K., J. Biol. Chem., 271 (1996) 15810.
48. Mancini, J.A., Vickers, P.J., O'Neill, G.P., Boily, C., Falgueyret, J.P. and Riendeau, D., Mol. Pharmacol., 51 (1997) 52.
49. Mancini, J.A., Riendeau, D., Falgueyret, J.P., Vickers, P.J. and O'Neill, G.P., J. Biol. Chem., 270 (1995) 29372.
50. Greig, G.M., Francis, D.A., Falgueyret, J.P., Ouellet, M., Percival, M.D., Roy, P., Bayly, C., Mancini, J.A. and O'Neill, G.P., Mol. Pharmacol., 52 (1997) 829.
51. Bhattacharyya, D.K., Lecomte, M., Rieke, C.J., Garavito, M. and Smith, W.L., J. Biol. Chem., 271 (1996) 2179.
52. So, O.Y., Scarafia, L.E., Mak, A.Y., Callan, O.H. and Swinney, D.C., J. Biol. Chem., 273 (1998) 5801.
53. Cignarella, G., Vianello, P., Berti, F. and Rossoni, G., Eur. J. Med. Chem., 31 (1996) 359.
54. Hendlich, M., Rippmann, F. and Barnickel, G. (unpublished), The ReLiBase System (Version 2.5), http://www2.ebi.ac.uk:8081/readme2.html.
55. Fukutake, M., Nakatsugi, S., Isoi, T., Takahashi, M., Ohta, T., Mamiya, S., Taniguchi, Y., Sato, H., Fukuda, K., Sugimura, T. and Wakabayashi, K., Carcinogenesis, 19 (1998) 1939.
56. Okajima, E., Denda, A., Ozono, S., Takahama, M., Akai, H., Sasaki, Y., Kitayama, W., Wakabayashi, K. and Konishi, Y., Cancer Res., 58 (1998) 3028.
57. Pedretti, A., Villa, A.M., Villa, L. and Vistoli, G., Farmaco, 52 (1997) 487.
58. Fabiola, G.F., Pattabhi, V. and Nagarajan, K., Bioorg. Med. Chem., 6 (1998) 2337.
59. Kollman, P., Chem. Rev., 93 (1993) 2395.
60. Åqvist, J., Medina, C. and Samuelsson, J.-E., Protein Eng., 7 (1994) 385.
61. Corpet, F., Nucleic Acids Res., 16 (1988) 10881.
62. SMOOFT routine, In Press, W.H., Flannery, B.P., Teukolsky, S.A. and Vetterling, W.T. (Eds.) Numerical Recipes, Cambridge University Press, Cambridge, U.K., 1989.